Inorg. Chem. **2004**, *43*, 7243–7249

Addition of $Pt(PBu^t_3)$ Groups to $Ru_5(CO)_{12}(\eta^6\text{-}C_6H_6)(\mu_5\text{-}C)$. Synthesis, Structures, and Dynamical Activity

Richard D. Adams,* Burjor Captain, Perry J. Pellechia, and Lei Zhu

Department of Chemistry and Biochemistry and the USC Nanocenter, University of South Carolina, Columbia, South Carolina 29208

Received July 23, 2004

The reaction of $Ru_5(CO)_{12}(\eta^6\text{-}C_6H_6)(\mu_5\text{-}C)$, **7**, with $Pt(PBu^t_3)_2$ yielded two products $Ru_5(CO)_{12}(\eta^6\text{-}C_6H_6)(\mu_6\text{-}C)[Pt(PBu^t_3)]$, **8**, and $Ru_5(CO)_{12}(\eta^6\text{-}C_6H_6)(\mu_6\text{-}C)[Pt(PBu^t_3)]_2$, **9**. Compound **8** contains a Ru_5Pt metal core in an open octahedral structure. In solution, **8** exists as a mixture of two isomers that interconvert rapidly on the NMR time scale at 20 °C, $\Delta H^{\ddagger} = 7.1(1)$ kcal mol^{-1}, $\Delta S^{\ddagger} = -5.1(6)$ cal mol^{-1} K^{-1}, and $\Delta G_{298}{}^{\ddagger} = 8.6(3)$ kcal mol^{-1}. Compound **9** is structurally similar to **8**, but has an additional $Pt(PBu^t_3)$ group bridging an Ru–Ru edge of the cluster. The two $Pt(PBu^t_3)$ groups in **9** rapidly exchange on the NMR time scale at 70 °C, $\Delta H^{\ddagger} = 9.2(3)$ kcal mol^{-1}, $\Delta S^{\ddagger} = -5(1)$ cal mol^{-1} K^{-1}, and $\Delta G_{298}{}^{\ddagger} = 10.7(7)$ kcal mol^{-1}. Compound **8** reacts with hydrogen to give the dihydrido complex $Ru_5(CO)_{11}(\eta^6\text{-}C_6H_6)(\mu_6\text{-}C)[Pt(PBu^t_3)](\mu\text{-}H)_2$, **10**, in 59% yield. This compound consists of a closed Ru_5Pt octahedron with two hydride ligands bridging two of the four Pt–Ru bonds.

Introduction

Heteronuclear (mixed-metal) cluster complexes have attracted attention for their use as precursors for the preparation of supported heterogeneous catalysts.[1–3] Mixed-metal clusters have also been shown to be good precursors for supported bimetallic nanoparticles.[4–11] Platinum−ruthenium carbonyl clusters have been shown to exhibit high catalytic activity for certain hydrogenation reactions when immobilized on mesoporous silica.[1,3a,b]

Recently, we have reported a series of new palladium- and platinum-containing bimetallic complexes formed by the addition of $M(PBu^t_3)$ groups, M = Pd and Pt, containing the sterically crowded PBu^t_3 ligand.[12] For example, $M(PBu^t_3)_2$, M = Pd and Pt, reacts with $Ru_3(CO)_{12}$ and $Ru_6(CO)_{17}(\mu_6\text{-}C)$ to yield the $M(PBu^t_3)$ adducts $Ru_3(CO)_{12}[Pd(PBu^t_3)]_3$, **1**, and $Ru_6(CO)_{17}(\mu_6\text{-}C)[M(PBu^t_3)]_2$, **2**, M = Pd, and **3**, M = Pt, respectively.[12a,h]

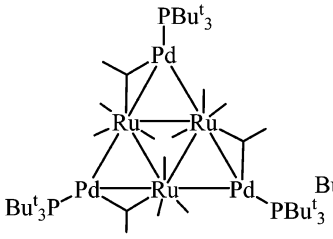

1

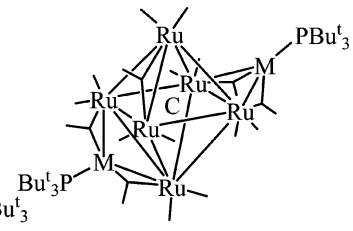

2 M = Pd
3 M = Pt

We have also shown that $Pd(PBu^t_3)_2$ and $Pt(PBu^t_3)_2$ react with $Ru_5(CO)_{15}(\mu_5\text{-}C)$ to afford the new complexes Ru_5-

* Author to whom correspondence should be addressed. E-mail: adams@mail.chem.sc.edu.

(1) (a) Thomas, J. M.; Johnson, B. F. G.; Raja, R.; Sankar, G.; Midgley, P. A. *Acc. Chem. Res.* **2003**, *36*, 20. (b) Thomas, J. M.; Raja, R.; Johnson, B. F. G.; Hermans, S.; Jones, M. D.; Khimyak, T. *Ind. Eng. Chem. Res.* **2003**, *42*, 1563. (c) Johnson, B. F. G. *Top. Catal.* **2003**, *24*, 147.

(2) (a) Sinfelt, J. H. *Bimetallic Catalysts: Discoveries, Concepts and Applications*; Wiley: New York, 1983. (b) Sinfelt, J. H. *Adv. Chem. Eng.* **1964**, *5*, 37. (c) Sinfelt, J. H. *Sci. Am.* **1985**, *253*, 90.

(3) (a) Thomas, J. M.; Raja, R.; Johnson, B. F. G.; O'Connell, T. J.; Sankar, G.; Khimyak, T. *Chem. Commun.* **2003**, 1126. (b) Raja, R.; Khimyak, T.; Thomas, J. M.; Hermans, S.; Johnson, B. F. G. *Angew. Chem., Int. Ed.* **2001**, *40*, 4638. (c) Hermans, S.; Raja, R.; Thomas, J. M.; Johnson, B. F. G.; Sankar, G.; Gleeson, D. *Angew. Chem., Int. Ed.* **2001**, *40*, 1211. (d) Raja, R.; Sankar, G.; Hermans, S.; Shephard, D. S.; Bromley, S.; Thomas, J. M.; Johnson, B. F. G.; Maschemeyer, T. *Chem. Commun.* **1999**, 1571.

(4) Toshima, N.; Yonezawa, T. *New J. Chem.* **1998**, 1179.

(5) Johnson, B. F. G. *Coord. Chem. Rev.* **1999**, *192*, 1269.

(6) Midgley, P. A.; Weyland, M.; Thomas, J. M.; Johnson, B. F. G. *Chem. Commun.* **2001**, 907.

(7) Nashner, M. S.; Frenkel, A. I.; Somerville, D.; Hills, C. W.; Shapley, J. R.; Nuzzo, R. G. *J. Am. Chem. Soc.* **1998**, *120*, 8093.

(8) Nashner, M. S.; Frenkel, A. I.; Adler, D. L.; Shapley, J. R.; Nuzzo, R. G. *J. Am. Chem. Soc.* **1997**, *119*, 7760.

(9) Shephard, D. S.; Maschmeyer, T.; Johnson, B. F. G.; Thomas, J. M.; Sankar, G.; Ozkaya, D.; Zhou, W.; Oldroyd, R. D.; Bell, R. G. *Angew. Chem., Int. Ed.* **1997**, *36*, 2242.

(10) Raja, R.; Sankar, G.; Hermans, S.; Shephard, D. S.; Bromley, S.; Thomas, J. M.; Johnson, B. F. G. *Chem. Commun.* **1999**, 1571.

10.1021/ic049004l CCC: $27.50
Published on Web 10/02/2004

$(CO)_{15}(C)[M(PBu^t_3)]$, **4**, M = Pd, and **5**, M = Pt, and $Ru_5(CO)_{15}(\mu_6\text{-}C)[Pd(PBu^t_3)]_2$, **6**. Compounds **4** and **5** both exist in solution as a mixture of open and closed isomers (e.g., **5a** and **5b**) that interconvert rapidly on the NMR time scale at room temperature.[12b,c] Compound **6** also engages in similar dynamical rearrangements that average the Pd groups on the NMR time scale at room temperature.[12c]

Compound **5** reacts with PhC_2H to yield the complex $PtRu_5(CO)_{13}(\mu_3\text{-}PhC_2H)(PBu^t_3)(\mu_5\text{-}C)$ that is capable of catalyzing the homogeneous hydrogenation of PhC_2H to styrene.[12e]

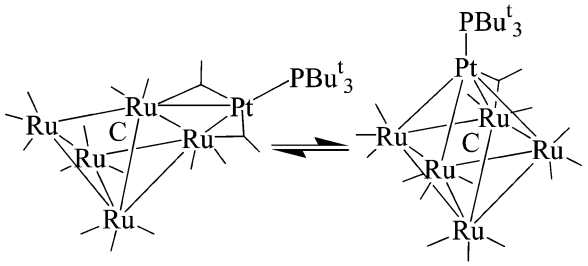

5a **5b**

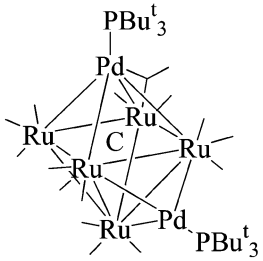

6

To explore the dynamical behavior of the $Pt(PBu^t_3)$ group in metal cluster complexes still further, we have now investigated the reaction of $Pt(PBu^t_3)_2$ with the benzene-containing pentaruthenium complex $Ru_5(CO)_{12}(\eta^6\text{-}C_6H_6)(\mu_5\text{-}C)$, **7**. Both mono- and diplatinum adducts $Ru_5(CO)_{12}(\eta^6\text{-}C_6H_6)(\mu_6\text{-}C)[Pt(PBu^t_3)]_n$, **8** and **9**, where $n = 1$ or $n = 2$, respectively, were obtained, and variable-temperature NMR studies show that the complexes are dynamically active by processes that involve rapid migration of the $Pt(PBu^t_3)$ groups about the Ru_5 cluster at room temperature. Additionally, compound **8** was found to react with hydrogen to yield the dihydrido cluster $Ru_5(CO)_{11}(\eta^6\text{-}C_6H_6)(\mu_6\text{-}C)[Pt(PBu^t_3)](\mu\text{-}H)_2$, **10**. The synthesis and characterization of compounds **8**−**10** along with the NMR studies that characterize the dynamical activity of the metal atoms in **8** and **9** are presented in this report.

Experimental Section

General Data. All reactions were performed under a nitrogen atmosphere. Reagent grade solvents were dried by the standard procedures and were freshly distilled prior to use. Infrared spectra were recorded on a Thermo Nicolet Avatar 360 FT-IR spectrophotometer. ^1H NMR and $^{31}P\{^1H\}$ NMR spectra were recorded on a Varian Mercury 400 spectrometer operating at 400.1 and 161.9 MHz, respectively. Variable-temperature $^{31}P\{^1H\}$ NMR spectra were recorded on a Varian Inova 500 spectrometer operating at 202.5 MHz. $^{31}P\{^1H\}$ NMR spectra were externally referenced against 85% H_3PO_4. Elemental analyses were performed by Desert Analytics (Tucson, AZ). Bis(tri-*tert*-butyl phosphine)platinum(0), $Pt(PBu^t_3)_2$, was obtained from Strem and was used without further purification. $Ru_5(CO)_{12}(\eta^6\text{-}C_6H_6)(\mu_5\text{-}C)$, **7**, was prepared according to the published procedure.[13] Product separations were performed by TLC in air on Analtech 0.25 and 0.5 mm silica gel 60 Å F_{254} glass plates.

Reaction of 7 with $Pt(PBu^t_3)_2$. $Pt(PBu^t_3)_2$ (12.3 mg, 0.021 mmol) was added to a solution of **7** (12.8 mg, 0.014 mmol) in 20 mL of CH_2Cl_2. The reaction mixture was stirred at room temperature for 1.25 h, after which the solvent was removed in vacuo. The products were separated by TLC using a 3:1 hexane/methylene chloride solvent mixture to yield in order of elution: 11.4 mg (62%) of $Ru_5(CO)_{12}(\eta^6\text{-}C_6H_6)(\mu_6\text{-}C)[Pt(PBu^t_3)]$, **8**, and 3.2 mg (13%) of $Ru_5(CO)_{12}(\eta^6\text{-}C_6H_6)(\mu_6\text{-}C)[Pt(PBu^t_3)]_2$, **9**. Spectral data for **8**, IR ν_{CO} (cm^{-1} in CH_2Cl_2): 2057 (m), 2038 (w, sh), 2022 (vs), 2007 (s), 1964 (w, sh), 1803 (w, br). ^1H NMR (in CD_2Cl_2) at room temperature: $\delta = 5.86$ (s, 6H, C_6H_6), 1.49 (d, 27H, CH_3, $^3J_{P-H} = 13$ Hz). $^{31}P\{^1H\}$ NMR (in CD_2Cl_2) at room temperature: $\delta = 98.97$ ($^1J_{Pt-P} = 6084$ Hz). Anal. Calcd: C, 28.01; H, 2.48. Found: C, 27.91; H, 2.67. Spectral data for **9**, IR ν_{CO} (cm^{-1} in CH_2Cl_2): 2042 (m), 2006 (vs), 1993 (s), 1957 (w, sh), 1800 (w, br). ^1H NMR (in CD_2Cl_2) at room temperature: $\delta = 5.52$ (s, 6H, C_6H_6), 1.51 (d, 27H, CH_3, $^3J_{P-H} = 13$ Hz). $^{31}P\{^1H\}$ NMR (in CD_2Cl_2) at room temperature: $\delta = 103.41$ ($^1J_{Pt-P} = 6100$ Hz). Anal. Calcd: C, 29.89; H, 3.47. Found: C, 29.95; H, 3.19.

Reaction of 7 with an Excess $Pt(PBu^t_3)_2$. $Pt(PBu^t_3)_2$ (38.4 mg, 0.064 mmol) was added to a solution of **7** (12.0 mg, 0.013 mmol) in 10 mL of CH_2Cl_2. The reaction mixture was heated to reflux for 3 h, after which the solvent was removed in vacuo. The products were separated by TLC using a 3:1 hexane/methylene chloride solvent mixture to yield in order of elution: 4.2 mg (25%) of $Ru_5(CO)_{12}(\eta^6\text{-}C_6H_6)(\mu_6\text{-}C)[Pt(PBu^t_3)]$, **8**, and 10.2 mg (46%) of $Ru_5(CO)_{12}(\eta^6\text{-}C_6H_6)(\mu_6\text{-}C)[Pt(PBu^t_3)]_2$, **9**.

Reaction of 8 with H_2. Compound **8** (13 mg, 0.010 mmol) dissolved in 15 mL of heptane was heated to reflux in the presence of a purge with hydrogen (1 atm) for 30 min. After the solvent was removed, the product was separated by TLC on silica gel by using a 3:1 hexane/CH_2Cl_2 solvent mixture to yield 7.5 mg (59%) of red $Ru_5(CO)_{11}(\eta^6\text{-}C_6H_6)(\mu_6\text{-}C)[Pt(PBu^t_3)](\mu\text{-}H)_2$, **10**. Spectral data for **10**, IR ν_{CO} (cm^{-1} in CH_2Cl_2): 2060 (m), 2030 (s), 2007 (s), 1993 (vs), 1950 (w, sh), 1800 (w, br). ^1H NMR (toluene-d_8 in ppm): $\delta = 4.51$ (s, 6H, C_6H_6), 1.25 (d, 27H, CH_3, $^3J_{P-H} = 13$ Hz), −14.93 (d, 2H, $^1J_{Pt-H} = 778$ Hz, $^2J_{P-H} = 8$ Hz). $^{31}P\{^1H\}$

(11) Shephard, D. S.; Maschmeyer, T.; Sankar, G.; Thomas, J. M.; Ozkaya, D.; Johnson, B. F. G.; Raja, R.; Oldroyd, R. D.; Bell, R. G. *Chem.*−*Eur. J.* **1998**, *4*, 1214.

(12) (a) Adams, R. D.; Captain, B.; Fu, W.; Smith, M. D. *J. Am. Chem. Soc.* **2002**, *124*, 5628. (b) Adams, R. D.; Captain, B.; Fu, W.; Pellechia, P. J.; Smith, M. D. *Angew. Chem., Int. Ed.* **2002**, *41*, 1951. (c) Adams, R. D.; Captain, B.; Fu, W.; Pellechia, P. J.; Smith, M. D. *Inorg. Chem.* **2003**, *42*, 2094. (d) Adams, R. D.; Captain, B.; Fu, W.; Smith, M. D. *J. Organomet. Chem.* **2003**, *682*, 113. (e) Adams, R. D.; Captain, B.; Zhu, L. *J. Am. Chem. Soc.* **2004**, *126*, 3042. (f) Adams, R. D.; Captain, B.; Fu, W.; Smith, J. L., Jr.; Smith, M. D. *Organometallics* **2004**, *23*, 589. (g) Adams, R. D.; Captain, B.; Pellechia, P. J.; Smith, J. L., Jr. *Inorg. Chem.* **2004**, *43*, 2695. (h) Adams, R. D.; Captain, B.; Fu, W.; Hall, M. B.; Manson, J.; Smith, M. D.; Webster, C. E. *J. Am. Chem. Soc.* **2004**, *126*, 5253. (i) Adams, R. D.; Captain, B.; Smith, M. D. *J. Cluster Sci.* **2004**, *15*, 139. (j) Adams, R. D.; Captain, B.; Fu, W.; Hall, M. B.; Smith, M. D.; Webster, C. E. *Inorg. Chem.* **2004**, *43*, 3921.

(13) Braga, D.; Grepioni, F.; Sabatino, P.; Dyson, P. J.; Johnson, B. F. G.; Lewis, J.; Bailey, P. J.; Raithby, P. R.; Stalke, D. *J. Chem. Soc., Dalton Trans.* **1993**, 985.

Table 1. Crystallographic Data for Compounds **8**, **9**, and **10**

	8		**9**	**10**
empirical formula	$PtRu_5PO_{12}C_{31}H_{33}$	$PtRu_5PO_{12}C_{31}H_{33}\cdot C_6H_6$	$Pt_2Ru_5P_2O_{12}C_{43}H_{60}\cdot{}^1/_2C_6H_6$	$PtRu_5PO_{11}C_{30}H_{35}$
formula weight	1328.98	1407.09	1765.43	1302.99
crystal system	monoclinic	monoclinic	orthorhombic	monoclinic
lattice parameters				
a (Å)	12.2809(6)	10.2939(11)	12.2868(3)	9.9622(6)
b (Å)	16.3600(7)	19.369(2)	25.0945(6)	18.5553(11)
c (Å)	19.0208(9)	11.1354(12)	35.1135(8)	21.1612(13)
β (deg)	101.8170(10)	105.122(2)	90	98.719(2)
V (Å^3)	3740.6(3)	2143.3(4)	10 826.6(4)	3866.5(4)
space group	$P2_1/c$ (No. 14)	$P2_1$ (No. 4)	*Pbca* (No. 61)	$P2_1/n$ (No. 14)
Z value	4	2	8	4
ρ_{calc} (g/cm^3)	2.360	2.180	2.166	2.238
μ (Mo Kα) (mm^{-1})	5.793	5.062	6.619	5.600
temperature (K)	296	296	296	296
$2\Theta_{max}$ (deg)	56.6	56.82	50.06	52.04
no. obs. ($I > 2\sigma(I)$)	8190	9091	8143	6028
no. parameters	460	514	621	450
GOF	1.025	1.003	1.228	1.072
max. shift in cycle	0.002	0.001	0.005	0.001
residuals:[a] R1, wR2	0.0222, 0.0179	0.0370, 0.0753	0.0482, 0.0985	0.0445, 0.0804
absorption correction	SADABS	SADABS	SADABS	SADABS
max/min	1.000/0.705	1.000/0.671	1.000/0.768	1.000/0.811
largest peak in final diff. map (e$^-$/Å^3)	0.810	1.176	1.290	1.217

[a] $R = \sum_{hkl}(||F_{obs}| - |F_{calc}||)/\sum_{hkl}|F_{obs}|$; $R_w = [\sum_{hkl}w(|F_{obs}| - |F_{calc}|)^2/\sum_{hkl}wF_{obs}^2]^{1/2}$, $w = 1/\sigma^2(F_{obs})$; GOF $= [\sum_{hkl}w(|F_{obs}| - |F_{calc}|)^2/(n_{data} - n_{vari})]^{1/2}$.

NMR (toluene-d_8 in ppm): $\delta = 86.62$ (s, 1P, $^1J_{Pt-H} = 4867$ Hz). Anal. Calcd: C, 27.65; H, 2.69. Found: C, 27.51; H, 2.87.

Crystallographic Analyses

Dark single crystals of **8** suitable for X-ray diffraction analyses were obtained by slow evaporation of solvent from a benzene/octane solvent mixture at 8 °C, from a diethyl ether solution at −25 °C, and from a hexane/methylenechloride solvent mixture at −25 °C. Dark red single crystals of **9** and **10** were obtained by slow evaporation from a benzene/octane solution at 8 °C. Each data crystal was glued onto the end of a thin glass fiber. X-ray intensity data were measured by using a Bruker SMART APEX CCD-based diffractometer using Mo Kα radiation ($\lambda = 0.71073$ Å). The raw data frames were integrated with the SAINT+ program by using a narrow-frame integration algorithm.[14] Correction for Lorentz and polarization effects was also applied with SAINT+. An empirical absorption correction based on the multiple measurement of equivalent reflections was applied using the program SADABS. All structures were solved by a combination of direct methods and difference Fourier syntheses and were refined by full-matrix least-squares on F^2, using the SHELXTL software package.[15] All non-hydrogen atoms were refined with anisotropic displacement parameters. Hydrogen atoms were placed in geometrically idealized positions and included as standard riding atoms during the least-squares refinements. Crystal data, data collection parameters, and results of the analyses are listed in Table 1.

The crystals of **8** were obtained in two crystalline modifications. The crystals obtained from diethyl ether solution and from hexane/methylenechloride solvent mixtures were the same and belong to the monoclinic crystal system. For these crystals, systematic absences in the intensity data were consistent with the space group $P2_1/c$. The structure was solved and suitably refined in this space group. The crystals of **8** obtained from a benzene/octane solvent mixture at 8 °C also belong to the monoclinic crystal system; the systematic absences in the intensity data for these crystals were consistent with either of the space groups $P2_1$ and $P2_1/m$. The structure could be solved only in the former space group. A molecule of benzene from the crystallization solvent cocrystallized with the complex. The solvent was included in the analysis and was satisfactorily refined with anisotropic thermal parameters.

Compound **9** crystallized in the orthorhombic crystal system. The space group *Pbca* was uniquely defined by the systematic absences observed in the data. One-half of a molecule of benzene from the crystallization solvent co-crystallized with the complex. The solvent was included in the analysis and was satisfactorily refined with anisotropic thermal parameters. For compound **10**, the systematic absences in the data identified the space group uniquely as $P2_1/n$. The two hydrido ligands were located, but were refined successfully only with geometric restraints.

NMR Calculations

Line-shape analyses were performed on a Gateway PC by using the program EXCHANGE written by R. E. D. McClung of the Department of Chemistry, University of Alberta, Edmonton, Alberta, Canada. For compound **8**, exchange rates were determined at 10 different temperatures in the temperature range from −90 to 20 °C. The activation parameters were determined from a least-squares fit of an Eyring plot ($\ln[hk/K_BT]$ vs $1/T$) by using the program Microsoft Excel 2002: $\Delta H^{\ddagger} = 7.1(1)$ kcal mol^{-1}, $\Delta S^{\ddagger} = -5.1(6)$ cal mol^{-1} K^{-1}, and $\Delta G_{298}{}^{\ddagger} = 8.6(3)$ kcal mol^{-1}. For compound **9**, exchange rates were determined at eight

(14) *SAINT+*, version 6.2a; Bruker Analytical X-ray System, Inc.; Madison, WI, 2001.
(15) Sheldrick, G. M. *SHELXTL*, version 6.1; Bruker Analytical X-ray Systems, Inc.: Madison, WI, 1997.

different temperatures in the temperature range from −50 to 35 °C. The activation parameters were determined from a least-squares fit of an Eyring plot (ln[hk/K_BT] vs $1/T$) using the program Microsoft Excel 2002: $\Delta H^{\ddagger} = 9.2(3)$ kcal mol^{-1}, $\Delta S^{\ddagger} = -5(1)$ cal mol^{-1} K^{-1}, and $\Delta G_{298}{}^{\ddagger} = 10.7(7)$ kcal mol^{-1}.

Results and Discussion

The reaction of the benzene coordinated pentaruthenium cluster $Ru_5(CO)_{12}(\eta^6\text{-}C_6H_6)(\mu_5\text{-}C)$, **7**, with $Pt(PBu^t_3)_2$ at room temperature gave two products $Ru_5(CO)_{12}(\eta^6\text{-}C_6H_6)(\mu_6\text{-}C)[Pt(PBu^t_3)]$, **8**, in 62% yield and $Ru_5(CO)_{12}(\eta^6\text{-}C_6H_6)(\mu_6\text{-}C)[Pt(PBu^t_3)]_2$, **9**, in 13% yield, see eq 1.

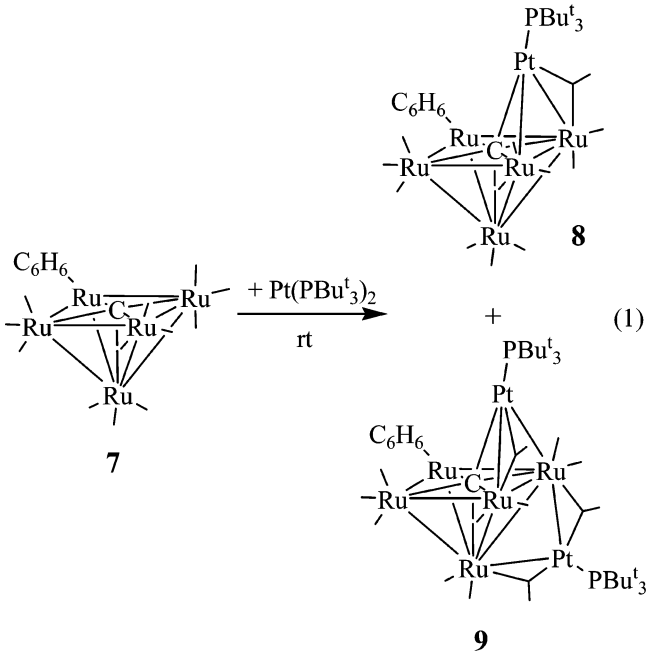

When an excess of $Pt(PBu^t_3)_2$ was used in the reaction, the yield of **9** was increased to 46%. Both products were characterized via IR, ^{1}H and ^{31}P NMR, single-crystal X-ray diffraction, and elemental analyses. Interestingly, we were able to obtain crystals of **8** in two different crystalline modifications, and the structures in both modifications were solved and satisfactorily refined. The molecular structure of **8** is very similar in both crystalline modifications, and an ORTEP diagram of the molecular structure is shown in Figure 1. Selected interatomic distances and angles for the molecule in both modifications are listed and compared in Table 2. Because there was no loss of CO from the starting material, compound **8** can be viewed as a $Pt(PBu^t_3)$ adduct of the parent complex **7**. The compound consists of a square-pyramidal cluster of five ruthenium atoms with a platinum atom located on the square base, but it is not symmetrically bonded to all four ruthenium atoms of the square base. In fact, there is significant bonding between the platinum atom and only two of the ruthenium atoms, Ru(1) and Ru(2), Pt(1)−Ru(1) = 2.9049(3) Å [2.8275(7) Å], and Pt(1)−Ru(2) = 2.8062(3) Å [2.7865(6) Å] (the quantity in brackets is the value for the molecule in the second crystalline modification), while the bonding to the other two ruthenium atoms Ru(4) and Ru(5) is small or nonexistent, Pt(1)−Ru(4) = 3.6283(3) Å [3.5897(8) Å] and Pt(1)−Ru(5) = 3.2307(3) Å [3.4314(7) Å]. In the closed isomer of the related compound $Ru_5(CO)_{15}(C)[Pt(PBu^t_3)]$, **5b**, there is significant bonding of the platinum atom to all four ruthenium atoms in the base of the Ru_5 square pyramid. The four Pt−Ru bond distances in **5b** range from 2.7966(5) to 3.1483(6) Å.[12c] The reason for the unsymmetrical bonding of the platinum atom on the Ru_4 square base in **8** is attributed to steric effects

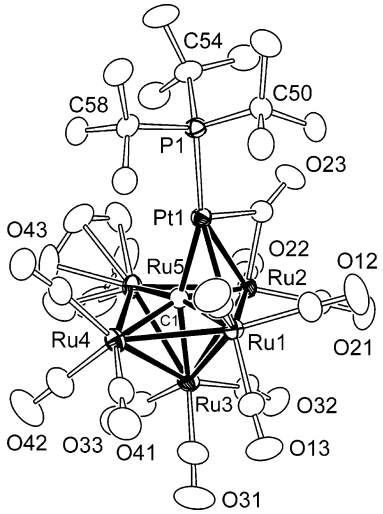

Figure 1. ORTEP diagram of the molecular structure of $Ru_5(CO)_{12}(\eta^6\text{-}C_6H_6)(\mu_6\text{-}C)[Pt(PBu^t_3)]$, **8**, showing 40% probability thermal ellipsoids.

Table 2. Selected Intramolecular Distances and Angles for the Two Polymorphs of Compound **8**[a]

(a) Distances (Å)

atoms	$P2_1/c$	$P2_1$
Pt(1)−Ru(1)	2.9049(3)	2.8275(7)
Pt(1)−Ru(2)	2.8062(3)	2.7865(6)
Pt(1)−Ru(4)	3.6283(3)	3.5897(8)
Pt(1)−Ru(5)	3.2307(3)	3.4314(7)
Pt(1)−P(1)	2.3335(7)	2.333(2)
Ru(1)−Ru(2)	2.9331(3)	2.9464(8)
Ru(1)−Ru(3)	2.8738(3)	2.7993(10)
Ru(1)−Ru(4)	2.8687(3)	2.8687(3)
Ru(2)−Ru(3)	2.7839(3)	2.8021(8)
Ru(2)−Ru(5)	2.8872(3)	2.8433(8)
Ru(3)−Ru(4)	2.7506(4)	2.7542(9)
Ru(3)−Ru(5)	2.8269(4)	2.8150(9)
Ru(4)−Ru(5)	2.8350(4)	2.8064(9)
Pt(1)−C(1)	2.139(3)	2.126(6)
Ru(1)−C(1)	2.099(3)	2.111(6)
Ru(2)−C(1)	2.118(3)	2.070(7)
Ru(3)−C(1)	2.239(3)	2.257(6)
Ru(4)−C(1)	2.087(3)	2.085(7)
Ru(5)−C(1)	1.925(3)	1.978(6)

(b) Angles (deg)

atoms	$P2_1/c$	$P2_1$
P(1)−Pt(1)−Ru(1)	135.84(2)	130.71(6)
Ru(2)−Pt(1)−Ru(1)	61.777(7)	63.309(18)
Ru(1)−Pt(1)−Ru(5)	81.227(7)	79.811(17)
Ru(2)−Pt(1)−Ru(4)	78.684(7)	78.611(16)
Ru(3)−Ru(1)−Pt(1)	96.341(9)	99.48(2)
Ru(3)−Ru(2)−Pt(1)	100.757(9)	100.41(2)
Pt(1)−C(1)−Ru(3)	159.26(14)	156.7(3)
Ru(5)−C(1)−Ru(1)	168.02(15)	162.6(3)

[a] Estimated standard deviations in the least significant figure are given in parentheses.

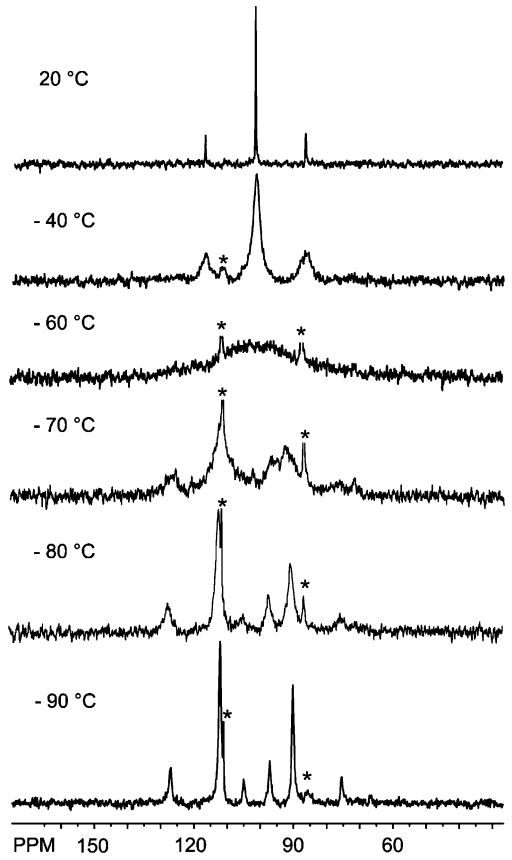

Figure 2. $^{31}P\{^1H\}$ NMR spectra at 202.5 MHz of compound **8** at various temperatures in toluene-d_8 solvent. The signal labeled with "*" is the impurity from compound **9**.

introduced by the benzene ligand that is coordinated to Ru(5) and the bulky tri-*tert*-butylphosphine ligand that is coordinated to the platinum atom. Curiously, the Pt−Ru distance to atom Ru(5) which contains the benzene ligand is actually slightly shorter than the Pt−Ru distance to Ru(4). This may be due to the presence of a bridging CO ligand on the Pt−Ru(2) bond which causes the Pt−Ru(2) to be shorter than the Pt−Ru(1) bond and in turn pulls the platinum atom to the Ru5 side of the cluster. The Ru−Ru bond distances lie in the range 2.7839(3)−2.9331(3) Å and are similar to those found in the parent cluster, **7**,[13] with the exception of the Ru(1)−Ru(2) bond which is slightly longer. This is because of the sharing of electrons in the Ru(1)−Ru(2) bond with the platinum atom. The carbide carbon atom lies in the center of the Ru$_4$ square base and is bonded to the platinum atom, Pt(1)−C(1) = 2.139(3) Å [2.126(6) Å].

The $^{31}P\{^1H\}$NMR spectra of **8** in solution at various temperatures are shown in Figure 2. The spectrum at − 90 °C shows two resonances at δ = 90.2 ($^1J_{Pt-P}$ = 5986 Hz) and δ = 112.1 ($^1J_{Pt-P}$ = 6050 Hz). Both resonances can be attributed to the phosphorus atom of a phosphine ligand. Both resonances exhibit large coupling to platinum (^{195}Pt, spin $^1/_2$, 33% natural abundance), indicating that the phosphorus atom is bonded to a platinum atom in each case. The presence of two phosphorus resonances suggests that compound **8** exists in solution as a mixture of two isomers. Compound **5** similarly exists as a mixture of two isomers in solution.[12b,c]

Scheme 1

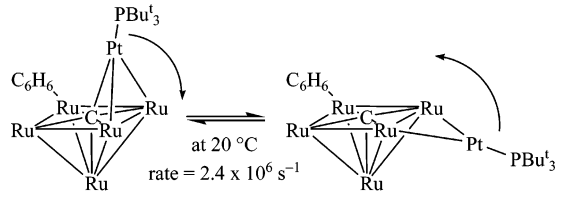

As the temperature is raised, both resonances of **8** begin to broaden and coalesce, reversibly. At 20 °C, the two resonances average into a single resonance at δ = 101.7 with large coupling to platinum, $^1J_{Pt-P}$ = 6161 Hz. Line-shape calculations were performed to determine the rates of interconversion at the various temperatures, from which the thermodynamic activation parameters have been obtained: $\Delta H^{\ddagger}$ = 7.1(1) kcal mol^{-1}, $\Delta S^{\ddagger}$ = −5.1(6) cal mol^{-1} K^{-1}, and $\Delta G_{298}^{\ddagger}$ = 8.6(3) kcal mol^{-1}.

It is not known at this time what the structure of the second isomer is, but on the basis of our previous work on the structures of **5**, it seems reasonable to assume that it is probably an open cluster where the Pt atom bridges only an edge of the base of the Ru$_5$ square pyramid, such as **8b** shown in Scheme 1.[12b,c] A mechanism to explain the interconversion of these two isomers, also shown in Scheme 1, would involve breaking of the Pt−C(1) bond and a shifting of the Pt(PBu$^t_3$) group to an Ru−Ru edge to form **8b**. The process occurs at a rate of 2 400 000 per second at 20 °C. This is considerably faster than the interconversion for the two isomers of compound **5** that was determined to be 24 000 per second at 20 °C. This can be explained in part by the differences between the bonding of the platinum atom to the Ru$_5$ cluster in **5a** and **8a**. In **5a**, the Pt atom is firmly bonded to all four Ru atoms of the Ru$_5$ square base. In compound **8**, the platinum atom is bonded to the carbido carbon atom and only two of the four ruthenium atoms; thus fewer bonds need to be broken for the Pt atom to shift to a Ru−Ru edge as in structure **8b**, and thus the process is more facile.

An ORTEP diagram of the molecular structure of compound **9** is shown in Figure 3. Selected interatomic distances and angles are listed in Table 3. Once again, there was no loss of a carbonyl ligand from **7**, and thus it can be viewed as a di-Pt(PBu$^t_3$) adduct of **7**. Like compound **8**, the structure of this compound also consists of a Ru$_5$Pt open octahedral-like arrangement of the metal atoms with a carbon atom in the center and a benzene ligand coordinated to Ru(4). The platinum atom Pt(1) is significantly bonded to only two of the ruthenium atoms, Ru(1) and Ru(2), Pt(1)−Ru(1) = 2.7744(8) Å, and Pt(1)−Ru(2) = 2.8959(8) Å, and the carbido carbon atom, Pt(1)−C(1) = 2.110(9) Å, while the bonding to the other two ruthenium atoms Ru(4) and Ru(5) is small or nonexistent, Pt(1)−Ru(4) = 3.3459(9) Å and Pt(1)−Ru(5) = 3.3518(8) Å. In addition, there is a second Pt(PBu$^t_3$) group that bridges the Ru(2)−Ru(3) bond. The Pt(2)−Ru(2) and Pt(2)−Ru(3) bond distances are 2.8460(8) and 2.7518(8) Å, respectively, and are similar to the Pt−Ru distances found in **3**: 2.7498(8)−2.8727(8) Å.[12h] Each of the Ru−Pt(2) bonds contains one bridging carbonyl ligand.

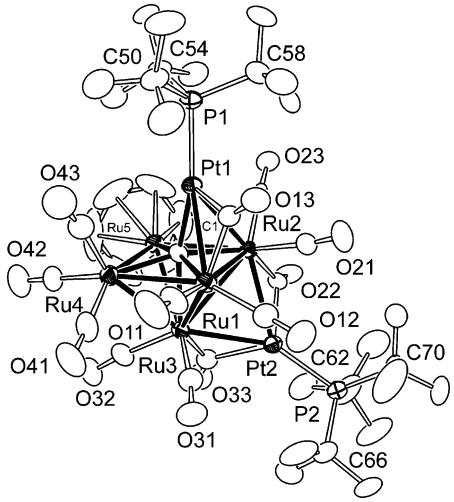

Figure 3. ORTEP diagram of the molecular structure of $Ru_5(CO)_{12}$-(η^6-C_6H_6)(μ_6-C)[$Pt(PBu^t_3)$]$_2$, **9**, showing 40% probability thermal ellipsoids.

Table 3. Selected Intramolecular Distances and Angles for Compounds **9** and **10**[a]

(a) Distances

compound **9**		compound **10**	
atoms	distance (Å)	atoms	distance (Å)
Pt(1)−Ru(1)	2.7744(8)	Pt(1)−Ru(1)	3.0293(6)
Pt(1)−Ru(2)	2.8959(8)	Pt(1)−Ru(2)	2.8402(7)
Pt(1)−Ru(4)	3.3459(9)	Pt(1)−Ru(4)	2.8348(6)
Pt(1)−Ru(5)	3.3518(8)	Pt(1)−Ru(5)	2.9801(7)
Pt(1)−P(1)	2.343(2)	Pt(1)−P(1)	2.3237(19)
Pt(2)−Ru(2)	2.8460(8)	Ru(1)−Ru(2)	2.9481(8)
Pt(2)−Ru(3)	2.7518(8)	Ru(1)−Ru(3)	2.7768(9)
Pt(2)−P(2)	2.339(2)	Ru(1)−Ru(4)	2.8797(8)
Ru(1)−Ru(2)	2.9357(10)	Ru(2)−Ru(3)	2.8505(8)
Ru(1)−Ru(3)	2.8362(11)	Ru(2)−Ru(5)	2.8898(9)
Ru(1)−Ru(4)	2.8764(11)	Ru(3)−Ru(4)	3.1713(9)
Ru(2)−Ru(3)	2.9480(10)	Ru(3)−Ru(5)	2.8095(9)
Ru(2)−Ru(5)	2.8448(10)	Ru(4)−Ru(5)	2.8707(8)
Ru(3)−Ru(4)	2.7732(11)	Pt(1)−C(1)	2.054(7)
Ru(3)−Ru(5)	2.7965(10)	Ru(1)−C(1)	2.109(6)
Ru(4)−Ru(5)	2.8714(11)	Ru(2)−C(1)	2.058(6)
Pt(1)−C(1)	2.110(9)	Ru(3)−C(1)	2.101(7)
Ru(1)−C(1)	2.093(8)	Ru(4)−C(1)	2.069(6)
Ru(2)−C(1)	2.093(9)	Ru(5)−C(1)	1.942(6)
Ru(3)−C(1)	2.229(9)		
Ru(4)−C(1)	2.083(9)		
Ru(5)−C(1)	1.945(8)		

(b) Angles

compound **9**		compound **10**	
atoms	angle (deg)	atoms	angle (deg)
P(1)−Pt(1)−Ru(1)	148.41(7)	P(1)−Pt(1)−Ru(1)	139.32(5)
Ru(1)−Pt(1)−Ru(2)	62.32(2)	Ru(2)−Pt(1)−Ru(1)	60.199(17)
Ru(1)−Pt(1)−Ru(5)	81.11(2)	Ru(5)−Pt(1)−Ru(1)	84.368(17)
Ru(2)−Pt(1)−Ru(4)	82.84(2)	Ru(4)−Pt(1)−Ru(2)	93.129(19)
Pt(1)−Ru(1)−Ru(3)	99.81(3)	Ru(3)−Ru(1)−Pt(1)	91.04(2)
Pt(1)−Ru(2)−Ru(3)	94.52(3)	Pt(1)−Ru(2)−Ru(3)	93.54(2)
Pt(1)−C(1)−Ru(3)	163.2(4)	Pt(1)−C(1)−Ru(3)	172.6(3)
Ru(5)−C(1)−Ru(1)	165.8(5)	Ru(5)−C(1)−Ru(1)	170.0(4)
P(2)−Pt(2)−Ru(2)	141.31(6)		
Ru(3)−Pt(2)−Ru(2)	63.53(2)		
Pt(2)−Ru(2)−Pt(1)	146.20(3)		

[a] Estimated standard deviations in the least significant figure are given in parentheses.

Variable-temperature $^{31}P\{^1H\}$ NMR spectra of **9** were also recorded and are shown in Figure 4. At −50 °C, the spectrum shows two resonances in a 1:1 ratio. These are attributed to

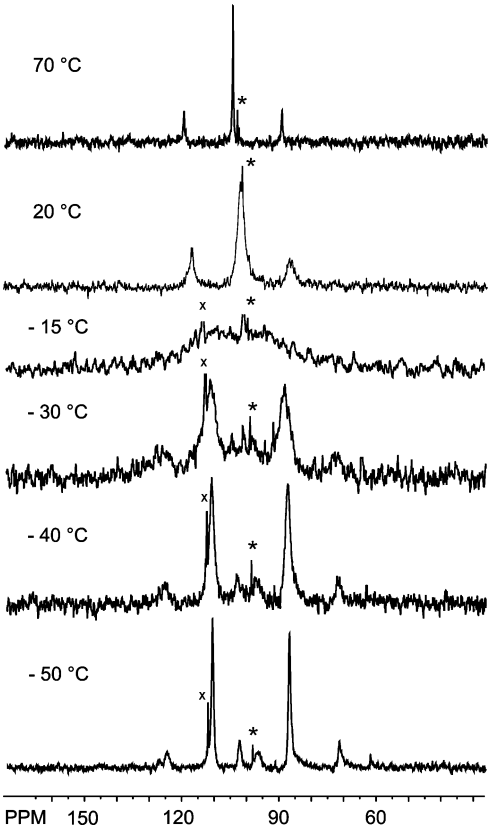

Figure 4. $^{31}P\{^1H\}$ NMR spectra at 202.5 MHz of compound **9** at various temperatures in toluene-d_8 solvent. The signal labeled with "*" is an impurity from **8**, and the signal labeled with "×" is an unidentified impurity.

Scheme 2

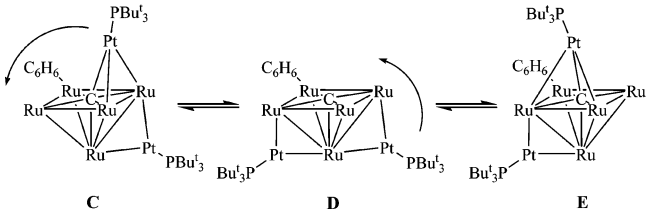

the two inequivalent PBu^t_3 ligands on Pt(1) and Pt(2), and each exhibits large one-bond coupling to platinum: $\delta = 87.6$ ($^1J_{Pt-P} = 6262$ Hz) and $\delta = 111.4$ ($^1J_{Pt-P} = 5695$ Hz). This spectrum is consistent with its solid-state structure. However, as the temperature is raised, the resonances broaden and coalesce reversibly. At 70 °C, the two resonances average into a sharp singlet at $\delta = 104.9$ with $^{31}P-^{195}Pt$ one-bond coupling maintained, $^1J_{Pt-P} = 6086$ Hz. Line-shape calculations were performed to determine the rates of exchange at the various temperatures, and these rates have provided the thermodynamic activation parameters for the exchange process: $\Delta H^{\ddagger} = 9.2(3)$ kcal mol^{-1}, $\Delta S^{\ddagger} = -5(1)$ cal mol^{-1} K^{-1}, and $\Delta G_{298}{}^{\ddagger} = 10.7(7)$ kcal mol^{-1}.

A proposed mechanism to explain the exchange of the $Pt(PBu^t_3)$ groups in **9** is shown in Scheme 2. This mechanism is based on the similar dynamic behavior exhibited by the compound $Ru_5(CO)_{15}(\mu_6$-C)[$Pd(PBu^t_3)$]$_2$, **6**, where two Pd-(PBu^t_3) groups exchange about a Ru_5 square pyramid.[12c] The two equivalent structures of **9** are represented as **C** and **E**. An intermediate such as **D** with two edge bridging $Pt(PBu^t_3)$ groups is produced when the $Pt(PBu^t_3)$ group on the Ru_5

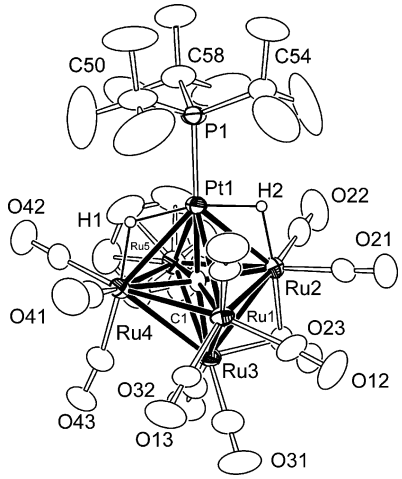

Figure 5. ORTEP diagram of the molecular structure of Ru$_5$(CO)$_{11}$-(η^6-C$_6$H$_6$)(μ_6-C)[Pt(PBu$^t_3$)](μ-H)$_2$, **10**, showing 40% probability thermal ellipsoids.

square base moves down to a Ru−Ru edge. From **D**, a Pt-(PBu$^t_3$) group could shift back up to the Ru$_5$ square base, resulting in the exchange of the two Pt(PBu$^t_3$) groups to give **E** or no exchange to give **C**.

The dynamical process occurring in compounds **8** and **9** is truly intramolecular. The fast exchange region for both compounds shows large ^{195}Pt−^{31}P one-bond coupling, indicating that there is no platinum−phosphine dissociation. Furthermore, there is no exchange between the two complexes in mixtures of the two, thus indicating that the Pt-(PBu$^t_3$) group does not dissociate.

When a heptane solution of compound **8** was heated to reflux in the presence of a hydrogen atmosphere, the new dihydrido complex Ru$_5$(CO)$_{11}$(η^6-C$_6$H$_6$)(μ_6-C)[Pt(PBu$^t_3$)]-(μ-H)$_2$, **10**, was formed in 59% yield, see eq 2.

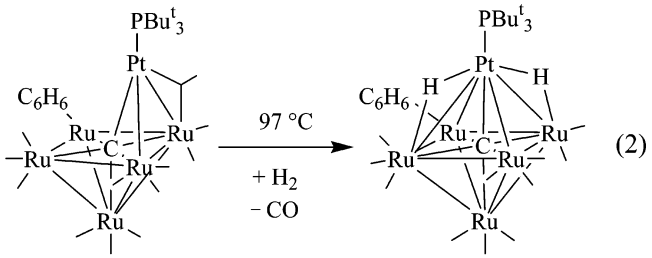

8 **10** (2)

Compound **10** was characterized by IR, ^{1}H and ^{31}P NMR, single-crystal X-ray diffraction, and elemental analyses, and an ORTEP diagram of its molecular structure is shown in Figure 5. Selected interatomic distances and angles are listed in Table 3. One carbonyl ligand was eliminated from **8**, and two hydride ligands were added to the cluster to form **10**. The structure of **10** is similar to that of the dihydrido complex Ru$_5$(CO)$_{14}$(μ_6-C)[Pt(PBu$^t_3$)](μ-H)$_2$, **11**, that has been obtained previously from the reaction of **5** with hydrogen.[12e] Compound **10** consists of an Ru$_5$Pt octahedron with a carbon atom in the center. The PBu$^t_3$ ligand is coordinated to the platinum atom, and the benzene ligand is coordinated to a ruthenium atom Ru(5). Unlike in compound **8**, the platinum atom is now bonded significantly to all four ruthenium atoms in the base of the Ru$_5$ square pyramid. The reason for this is probably due to the presence of the bridging hydride ligands that strengthen the Pt−Ru bonds. The two hydrido ligands bridge two oppositely positioned Pt−Ru bonds. Interestingly, the hydride bridged Pt−Ru bonds, Pt(1)−Ru(2) = 2.8402-(7) Å, and Pt(1)−Ru(4) = 2.8348(6) Å, are significantly shorter than the unbridged Pt−Ru bonds, Pt(1)−Ru(1) = 3.0293(6) Å, and Pt(1)−Ru(3) = 2.9801(7) Å. A similar shortening effect was observed for the hydride bridged Pt−Ru bonds in **11**. This is contrary to the usual bond lengthening effects that have been observed for hydride bridged metal−metal bonds in most other hydride-containing cluster complexes.[16] The two hydride ligands in **10** are equivalent and appear as a single resonance, $\delta = -14.93$, in the ^{1}H NMR spectrum that exhibits one-bond coupling to platinum and two-bond coupling to the phosphorus atom ($^1J_{Pt-H}$ = 778 Hz, $^2J_{P-H}$ = 8 Hz).

When compound **9** was allowed to react with hydrogen (1 atm) at 97 °C, compound **10** was obtained in low yield along with a few other minor products that were not characterized.

These results further extend the range of new Pt(PBu$^t_3$) cluster complex derivatives. As with compound **5**, compounds **9** and **10** further demonstrate the ability of Pt(PBu$^t_3$) groups to migrate readily about the surface of metal cluster complexes and provide still another example of the "cluster-surface" analogy[17] with regard to migration of metal atoms on metal surfaces by the mechanism of "atom hopping".[12b,c,18]

Acknowledgment. This research was supported by the Office of Basic Energy Sciences of the U.S. Department of Energy under Grant DE-FG02-00ER14980. We thank Strem for donation of a sample of Pt(PBu$^t_3$)$_2$ and the USC Nanocenter for financial support.

Supporting Information Available: Crystallographic data in CIF format. This material is available free of charge via the Internet at http://pubs.acs.org.

IC049004L

(16) Teller, R. G.; Bau, R. *Struct. Bonding* **1981**, *41*, 1.
(17) (a) Muetterties, E. L. *Chem. Rev.* **1979**, *79*, 93. (b) Muetterties, E. L. *Chem. Soc. Rev.* **1982**, *11*, 283. (c) Muetterties, E. L. *Surv. Prog. Chem.* **1983**, *10*, 61. (d) Albert, M. R.; Yates, J. T., Jr. *The Surface Scientist's Guide to Organometallic Chemistry*; American Chemical Society: Washington, DC, 1987. (e) Xu, X.; Wang, N.; Zhang, Q. *Bull. Chem. Soc. Jpn.* **1996**, *69*, 529.
(18) (a) Kellogg, G. L. *Surf. Sci. Rep.* **1994**, *21*, 1. (b) Chang, C. M.; Wei, C. M.; Hafner, J. *J. Phys.: Condens. Matter* **2001**, *13*, L321.